Remote Sensing of Environment 167 (2015) 218–228

Contents lists available at ScienceDirect

Remote Sensing of Environment

journal homepage: www.elsevier.com/locate/rse

Remote monitoring of giant kelp biomass and physiological condition: An evaluation of the potential for the Hyperspectral Infrared Imager (HyspIRI) mission

Tom W. Bell [a,*,1], Kyle C. Cavanaugh [b,1], David A. Siegel [a]

[a] Earth Research Institute, University of California, Santa Barbara, CA 93106, USA
[b] Department of Geography, University of California, Los Angeles, CA 90095, USA

ARTICLE INFO

Article history:
Received 31 May 2014
Received in revised form 14 May 2015
Accepted 14 May 2015
Available online 26 May 2015

Keywords:
HyspIRI
Landsat
AVIRIS
Giant kelp
Hyperspectral
Wavelet analysis
Macrophyte
Coastal ecology

ABSTRACT

This study examines the potential of the Hyperspectral Infrared Imager (HyspIRI) mission for monitoring the biomass and physiological condition of giant kelp forests on local to global scales. Giant kelp is a highly dynamic foundation species that supports an ecologically and economically important ecosystem found throughout the globe. Satellite, airborne, and field data are used to evaluate the suitability of HyspIRI's spatial, temporal, and spectral coverage for capturing variability in giant kelp biomass and physiological state. We analyze a 28-year time series of giant kelp biomass derived from Landsat satellite imagery in order to identify the dominant temporal modes of variability in giant kelp biomass using the California coast as a model region likely to be relevant to other regions of the globe. Temporal variability in California kelp canopy biomass is compared to the expected availability of cloud-free HyspIRI Visible Shortwave Infrared (VSWIR) views for regions of the world that contain giant kelp populations. Spectral variability is explored by assessing how changes in the physiological condition of giant kelp canopy are exhibited in the reflectance and transmittance of kelp fronds. We compare chlorophyll *a* to carbon ratios (Chl:C) of kelp fronds collected off the coast of California to laboratory and airborne measurements of hyperspectral reflectance in order to develop metrics of kelp physiological condition.

The seasonal cycle dominates giant kelp canopy biomass temporal variability. However, the strength and timing of this cycle varies in both space and time. Our projections of cloud-free HyspIRI coverage indicate that the sensor will be able to capture at least 1 cloud free view each season for nearly all of the global giant kelp habitats, thereby illustrating that HyspIRI will resolve the dominant seasonal cycles in giant kelp biomass. A novel spectral index developed here from field observations explained 76% of the variance in Chl:C and was applied to hyperspectral aircraft observations. These results demonstrate that the spatial, temporal, and spectral coverage provided by HyspIRI has the potential to provide new insights into the ecology and biophysiology of giant kelp.

© 2015 Elsevier Inc. All rights reserved.

1. Introduction

Giant kelp (*Macrocystis pyrifera*) is the foundation species for a highly productive marine ecosystem, and has long been recognized as an important economic and ecological resource (Leet, Dewees, Klingbeil, & Johnson, 2001; Mann, 1973). Importantly, giant kelp is considered an ecosystem engineer and its presence facilitates the emergence of the kelp forest ecosystem (Graham, 2004). The holdfasts, mid-water fronds, and surface canopy of giant kelp provide habitat structure throughout the water column for a highly diverse assemblage of algae, invertebrates, and fishes (Foster & Schiel, 1985; Graham, Vasquez, & Buschmann, 2007). In addition, *Macrocystis*-derived primary productivity supplies energy to the kelp forest food web via both direct grazing of kelp and the utilization of kelp detritus and exudates (Graham, Halpern, & Carr, 2008). Giant kelp is highly dynamic and individual kelp fronds and entire "plants" have short lifespans (3–5 months and 2–3 years respectively; Rodriguez, Rassweiler, Reed, & Holbrook, 2013), due largely to age-related senescence and wave-induced mortality (Graham et al., 2007). However, these high rates of mortality are balanced by high growth rates (maximum growth rates are ~2% of total biomass per day), which results in a standing biomass that turns over 6–7 times per year (Reed, Rassweiler, & Arkema, 2008).

Efforts to monitor the location, size, and biomass of giant kelp forests were established in response to the human harvest of giant kelp and exploitation of the ecosystems that kelp forests support. Giant kelp is anchored to the seafloor, but it develops a dense floating canopy that

* Corresponding author at: 5843 Ellison Hall, University of California, Santa Barbara, CA 93106, USA. Tel.: + 1 619 857 1233.
E-mail addresses: thomas.bell@lifesci.ucsb.edu (T.W. Bell), kcavanaugh@geog.ucla.edu (K.C. Cavanaugh).
[1] Authors contributed equally to this work.

http://dx.doi.org/10.1016/j.rse.2015.05.003
0034-4257/© 2015 Elsevier Inc. All rights reserved.

is distinctive when viewed from above and is therefore one of the few types of subtidal algae amenable to aerial monitoring (Jamison, 1971). The reflectance of this surface canopy is similar to that of terrestrial vegetation, with high near infrared reflectance (NIR), and so it can be easily differentiated from water using multispectral imagery (Jensen, Estes, & Tinney, 1980). Large-scale aerial surveys of giant kelp of the California, USA, coastline were initiated in the 1950s by ISP Alginates, a major kelp harvesting firm (McPeak, Glantz, & Shaw, 1988). During these surveys a trained observer would fly along the California coastline in a small plane and visually estimate kelp biomass. In 1967 an annual aerial survey was initiated to track the maximum areal extent of giant kelp canopy along the coast of Southern California using infrared photographs (North, 1991). In 1989 the California Department of Fish and Game began conducting similar kelp surveys along the entire California coastline (Veisze, Kilgore, & Lampinen, 2001) and these surveys continue today. This and associated aerial time series have been used for both ecological research and resource management purposes. North, James, and Jones (1993) used a 25-year time series to study how maximum annual canopy extent was affected by climate oscillations, storms, and human impacts, such as waste-water discharge. The spatial variability of the effect of wave disturbance on kelp, and the spatial and temporal dynamics of canopy coverage around the Monterey Peninsula were assessed using aerial photographs (Donnellan, 2004; Graham et al., 1997). Data from aerial surveys were used to study the drivers of the spatial persistence of giant kelp in order to evaluate an existing network of marine protected areas around Catalina Island, CA (Bushing, 1997). These data were also used by state agencies to assess the state of southern California's mainland kelp forests (SCCWRP, 2011) and regulate the commercial and recreational harvest of giant kelp (Larson & McPeak, 1995).

As data from Earth observing spaceborne platforms became increasingly available, their utility in measuring the extent of giant kelp canopies was assessed by comparison to aerial photo surveys. Assessments of kelp canopy area from Landsat 1 and 2 images were highly correlated to assessments from aerial photographs, but the Landsat methods consistently underestimated canopy area (Jensen et al., 1980). Augenstein, Stow, and Hope (1991) built on this work by developing a standardized methodology for identifying kelp canopy on 20 m resolution SPOT satellite imagery. They also found that NIR radiance increased as a function of increasing density, which enabled them to create thematic maps of kelp canopy density. A subsequent study using SPOT images found that areal extent of less dense kelp canopies was underestimated compared to annual infrared photographs due to a lack of contrast between kelp canopy and turbid waters (Deysher, 1993).

Aerial extent is one measure of giant kelp abundance, but kelp biomass determinations are more useful for estimating primary productivity (Reed et al., 2008), quantifying harvestable kelp stocks, and estimating resources available to kelp forest communities. Stekoll, Deysher, and Hess (2006) made the first remote estimates of kelp biomass for two other species of canopy forming kelps, *Nereocystis luetkeana* and *Alaria fistulosa* using high-resolution multispectral aerial imagery. Cavanaugh, Siegel, Kinlan, and Reed (2010) found that normalized difference vegetation index values from 10 m resolution SPOT satellite imagery were strongly correlated with diver observations of giant kelp biomass along the coast of Santa Barbara. While these studies demonstrated the feasibility of remote monitoring of kelp biomass, they only analyzed a few image dates (2 to 13 dates) and had relatively small study areas (5 to 60 km) and so their utility for examining spatiotemporal variability in giant kelp abundance was limited.

A large-scale (~1500 km), long-term (nearly 30 year) giant kelp canopy biomass data set has recently been created using Landsat 5 Thematic Mapper (TM) satellite imagery (Cavanaugh, Siegel, Reed, & Dennison, 2011). The use of open access Landsat 5 TM images allowed canopy biomass estimates to be made across all of southern California every 1–2 months from 1984–2011. The spatial and temporal resolution and extent of the Landsat data enabled the drivers of seasonal, annual, and decadal fluctuations in kelp abundance and productivity to be examined across a range of spatial scales (Bell, Cavanaugh, Reed, & Siegel, in press; Cavanaugh et al., 2011, 2013; Reed et al., 2011), characterize the metapopulation dynamics of kelp forest ecosystems (Castorani et al., in press; Cavanaugh, Siegel, Raimondi, & Alberto, 2014), and explore the role of disturbance in structuring kelp forest food webs (Byrnes et al., 2011).

As described above, remotely sensed data has been used to quantify kelp canopy extent and biomass; however, remote assessments of the physiological condition of giant kelp, such as the photosynthetic pigment (chlorophyll *a*) to carbon content ratio (Chl:C; Geider, 1987; Geider, MacIntyre, & Kana, 1997), have not yet been made. Values of Chl:C represent an integrated measure of an organism's physiological investment in the photosynthetic apparatus and vary depending on environmental conditions, such as light, available nutrients, and temperature. In marine phytoplankton, values of Chl:C range from 0.001 to >0.06 mg mg^{-1} and have been used to assess phytoplankton community physiological status and to estimate rates of phytoplankton net primary production from remotely sensed images (Behrenfeld, Boss, Siegel, & Shea, 2005). The photosynthetic pigment state of giant kelp responds to changes in environmental conditions such as light and nutrient levels, with low light, high nutrient conditions increasing pigment concentrations (Shivji, 1985), while structural carbon content remains relatively constant (Brzezinski, Reed, & Harrer, 2013). During times of low nutrient conditions, giant kelp blades become lighter in color and photosynthetic rates decline (Clendenning, 1971), and changes in giant kelp photosynthetic rates have been tied to changes in the chlorophyll *a* pigment (Wheeler, 1980). The spatial and temporal variability of nutrient and light conditions throughout the range of giant kelp is high due to changing oceanographic conditions (Bell et al., in press; Parnell, Miller, Lennert-Cody, Dayton, & Carter, 2010). It is expected that the spatiotemporal variability of nutrient (nitrate) and light availability across the large latitudinal range of giant kelp will lead to a dynamic physiological state in the surface canopy. Data on pigment to carbon ratios would allow researchers to better estimate the productivity of giant kelp, link performance to environmental conditions, and explore other ecological questions. Hyperspectral sensors have the potential for observing changes in the physiological state of giant kelp through assessment of canopy Chl:C from satellite orbit. Recent studies using hyperspectral imaging on marine macroalgae have been limited to mapping and classification on local scales, at a single or a few time points, due to high cost and limited availability of airborne data (Gagnon, Scheibling, Jones, & Tully, 2008; Volent, Johnsen, & Sigernes, 2007). A spaceborne hyperspectral sensor could be used to create a high quality, consistent time series, with a temporal resolution sufficient to monitor changes in the local to global scale biomass distribution and physiological condition of this dynamic organism.

In this study, we investigate the utility of the HyspIRI mission to fulfill these goals by exploring the following questions: (1) Will the 19-day revisit time of HyspIRI adequately capture giant kelp forest biomass and physiological condition dynamics? (2) Will the spectral resolution of HyspIRI allow for the assessment of physiological condition of the giant kelp canopy? (3) What new questions will HyspIRI allow researchers to answer concerning the ecological role of this globally distributed ecosystem engineer?

2. Methods

2.1. Expected cloud-free HysPIRI coverage of global giant kelp habitat

We assessed the potential of HyspIRI to provide cloud-free coverage of global giant kelp habitat by using a Terra MODIS 5 km daytime cloud mask dataset to determine the percent of MODIS views that were cloud free between 2001 and 2010 (data provided by Mercury et al., 2012). Giant kelp habitat was identified using the global distribution map

provided in Fig. 1 of Graham et al. (2007). Within the regions that contained kelp habitat we identified the 5 km grid cells of the Terra MODIS cloud coverage map that intersected the coastline. Coastline data was obtained from the intermediate resolution version of NOAA's Global, Self-consistent, Hierarchical, High-resolution Shoreline Database (Wessel & Smith, 1996). We separated global kelp habitat into 8 regions (western North America from the Gulf of Alaska to San Francisco Bay, western North America from San Francisco Bay to Baja California, South America, the Falkland Islands, South Africa, Tasmania, New Zealand, and the sub-Antarctic Islands) and calculated the mean percent cloudiness between 2001 and 2010 for each region.

The mean number of cloud-free views of each region that the HyspIRI VSWIR sensor will obtain each season was estimated by multiplying the fraction of cloudy MODIS images in a season by the total number of HyspIRI VSWIR views during that season. Assuming a 19-day revisit time for the HyspIRI VSWIR sensor, the total number of views during a season will be 4.789 (91 days in a season divided by the 19 day revisit time). The actual revisit time for a given location varies by latitude and will impact the true probability of cloud-free coverage (Mercury et al., 2012). To evaluate the potential of Landsat 8 (or a sensor with similar orbital characteristics) to complement HyspIRI's kelp monitoring, we also calculated the expected number of cloud-free views each season from Landsat 8 (16-day revisit time).

2.2. Study area

We analyzed the dynamics of giant kelp biomass along the coast of California from Año Nuevo to the USA/Mexico border. This region experiences a great deal of spatial and temporal variability in environmental conditions that control kelp abundance. Sea surface temperature, nutrient conditions, and wave energy are all characterized by pronounced seasonal cycles (Di Lorenzo, 2003; Harms & Winant, 1998; Lynn & Simpson, 1987; Seymour, 2011). Storms in the North Pacific create sporadic large northwest swell events with significant wave heights (H_s) greater than 4 m during the winter months, while summer months experience smaller southern swells (maximum H_s ~ 2–3 m; O'Reilly & Guza, 1993). Coastal upwelling is strongest during the spring and causes nutrient levels to be highest during these months. Spatially, Point Conception represents a natural oceanographic boundary. Strong and persistent upwelling north of Point Conception keeps nutrient levels high throughout the year, while vertical stratification during the summer and fall leads to warmer temperatures and lower nitrate levels south of Point Conception (McPhee-Shaw et al., 2007). Wave energy is also generally greater north of Pt. Conception throughout the year (Bell et al., in press; Foster & Schiel, 1985; Reed et al., 2011; Seymour, 2011), as this coastline is exposed to both powerful winter northwest swells as well as weaker summer southern swells. On annual to decadal timescales, large-scale oceanographic cycles such as the Pacific Decadal Oscillation (PDO), El Niño-Southern Oscillation (ENSO), and North Pacific Gyre Oscillation (NPGO) influence seawater temperatures, nutrient levels, and storm patterns (Di Lorenzo et al., 2010; Mantua & Hare, 2002; Seymour, 1998), which can have a major impact on giant kelp populations (Bell et al., in press; Dayton & Tegner, 1984; Parnell et al., 2010). We performed further analysis of the physiological condition of the canopy of kelp forests located along the mainland coast of the Santa Barbara Channel (SBC) by conducting a field sampling campaign and collecting AVIRIS imagery. Bathymetry data was estimated for these kelp forests using bathymetry grids from the National Geophysical Data Center Coastal Relief Model (3 arc sec; Divins & Metzger, 2009).

2.3. Landsat estimates of kelp canopy biomass

Multispectral Landsat 5 Thematic Mapper (TM) imagery was used to monitor kelp canopy biomass along the coast of California from Año Nuevo to the USA/Mexico border throughout the extent of that satellite mission's useful lifetime (1984 to 2011). The methods used to process and calibrate the Landsat 5 TM imagery into giant kelp canopy biomass are detailed in Cavanaugh et al. (2011). In brief, kelp canopy fractional cover was estimated for each atmospherically corrected Landsat 5 TM scene using multiple endmember spectral mixing analysis (MESMA; Roberts et al., 1998). We modeled pixel reflectance as a linear combination of two endmembers: water and kelp canopy. Thirty seawater endmembers were selected from each Landsat scene in order to account for variability in water spectra due to varying sediment and phytoplankton chlorophyll concentrations, sunglint, etc. A single, image-based kelp endmember was used for all images and the MESMA model was used to determine each pixel's kelp fraction. A linear relationship was found between diver estimated kelp canopy biomass and Landsat pixel kelp fraction and this relationship was used to estimate kelp canopy biomass from the Landsat imagery (Cavanaugh et al., 2011). Canopy biomass was estimated from Landsat images taken approximately once every 1 to 3 months and the canopy biomass time series was interpolated onto a regular seasonal (3-month) time scale for the entire domain using a cubic spline (Bell et al., in press). Canopy biomass observations were binned into 500 m alongshore coastline segments by assigning each pixel of kelp canopy to the closest coastline segment.

2.4. AVIRIS imagery

The Airborne Visible/Infrared Imaging Spectrometer (AVIRIS) provides hyperspectral images of upwelling spectral radiance in 224 contiguous, 10 nm bands (400–2500 nm). Orthocorrected AVIRIS images, with an 11 km swath width, were collected on April 11, 2013 over the SBC as part of the HyspIRI Airborne Campaign (http://hyspiri.jpl.nasa.gov/airborne). We analyzed AVIRIS imagery that covered approximately 20 km of the coastline near Santa Barbara, CA. Standard level 2 reflectance products at an 18 m spatial resolution were used. Apparent surface reflectance of these images was retrieved using the Atmosphere Removal Algorithm (ATREM) from radiance data (Gao, Heidebrecht, & Goetz, 1993). Spectra were resampled using nearest neighbor sampling to a regular 18 m grid. Fractional kelp cover was determined for each pixel using MESMA as described previously.

2.5. Laboratory kelp blade analysis

Giant kelp surface blade reflectance, transmittance, and chlorophyll *a* concentration were measured from the Mohawk (34.394 N, 119.730 W), Arroyo Burro (34.400 N, 119.745 W), and Arroyo Quemado (34.468 N, 120.119 W) kelp forests in the SBC each month between August 2012 and December 2013. Santa Barbara Coastal Long Term Ecological Research project (SBC LTER) divers collected 15 mature surface blades, which were approximately the same age as they were all located 2 m from a growing frond tip. Epibionts were not removed from the blades during reflectance and transmittance measurements, however coverage was minimal throughout the sampling period. Reflectance and transmittance were measured for each blade between 350 and 800 nm range using a Shimadzu UV 2401PC spectrometer with an integrating sphere attachment. Concentrations of chlorophyll *a* were measured for each blade following Seely, Duncan, and Vidaver (1972). A separate sample of kelp tissue from each blade was dried at 60 °C, and carbon content was determined from a pooled sample using a Carlo-Erba Flash EA 1112 series elemental analyzer (Thermo-Finnigan Italia), calibrated against an aspartic acid standard.

2.6. Chl:C algorithm development

Chlorophyll *a* absorbs light in the red and blue regions of the visible spectrum, however carotenoids, such as fucoxanthin, also absorb in the blue region (Seely et al., 1972). Due to this pigment overlap, we chose to focus on the chlorophyll *a* absorption feature in the red region, centered at 665 nm. The prediction of chlorophyll *a* content from reflectance in

terrestrial plants has focused on variability around the red edge near 700 nm, due to the overlap of absorption features of chlorophylls *a* and *b* at wavelengths less than 665 nm (Sims & Gamon, 2002). However, giant kelp lacks the chlorophyll *b* pigment, and the accessory pigment chlorophyll *c* is usually found in relatively small concentrations and absorbs at higher energy wavelengths than chlorophyll *b*. This further separation of the absorption features of chlorophylls *a* and *c* and allows for the examination of both sides of the chlorophyll *a* absorption feature at 665 nm for its relationship to chlorophyll *a* content (Wheeler, 1980).

To determine if Chl:C could be estimated from AVIRIS imagery, laboratory reflectance was degraded to AVIRIS bands by taking the mean of reflectance in each AVIRIS band. The change between each band's reflectance value was measured as the slope of apparent absorbance (i.e., first derivative of pseudo absorbance δ(Log 1/R); Yoder & Pettigrew-Crosby, 1995). These slopes were correlated to the measured Chl:C of surface canopy blades from all sampling dates using linear and exponential fits. The optimized wavelengths for Chl:C prediction were identified as the region where the slope of apparent absorbance explained the highest amount of variability in blade Chl:C. The optimal spectral predictor of Chl:C from AVIRIS degraded laboratory reflectance was the first derivative of pseudo absorbance at 658–667 nm (Fig. 1a) using an exponential relationship (Eq. (1)),

$$\text{Chl} : \text{C} = 0.0353e^{-7.53x} \quad (1)$$

where x is equal to the slope of pseudo absorbance between 658 and 667 nm. While first derivative of pseudo absorbance at 658–667 nm was selected as the optimal metric, we found that a large amount of variance was also explained in the blue and red regions of the spectrum (n = 40; Fig. 1a). To validate pigment concentration predictions, we used a 5-fold cross validation, in which 4/5 of the dataset was used for training and 1/5 for prediction, repeated 5 times. The predictions accounted for 76% of the observed variance for Chl:C ($p < 0.001$; Fig. 1b). Laboratory reflectance, normalized at 667 nm, demonstrated that increased spectral slope between 658 and 667 nm was associated with decreased Chl:C (Fig. 1c). This relationship for Chl:C was used to predict the spatial distribution of giant kelp physiological condition using an AVIRIS image collected on April 11, 2013. By comparing these laboratory reflectance spectra to AVIRIS atmospherically corrected reflectance spectra, also normalized at 667 nm, it was apparent that the shape and magnitudes of reflectance in this region of the spectrum were similar (Image date 4/11/2013; Fig. 1d).

2.7. Statistical analyses

Wavelet analysis was used to identify the dominant periodicities in the Landsat giant kelp canopy biomass time series and track how those different periodic components changed over time. Wavelet analysis is a useful tool for examining nonstationary processes such as transient population dynamics (Cazelles et al., 2008). This is particularly relevant for giant kelp populations along the coast of California, as these populations appear to switch between different dynamics on multidecadal scales in response to low frequency climate modes (Bell et al., in press; Cavanaugh et al., 2011; Dayton, Tegner, Edwards, & Riser, 1999; Parnell et al., 2010). The Morlet basis function was used to calculate wavelet transforms returning information about both amplitude and phase, making it suitable for capturing oscillatory behavior in time series data (Torrence & Compo, 1998). With this function we

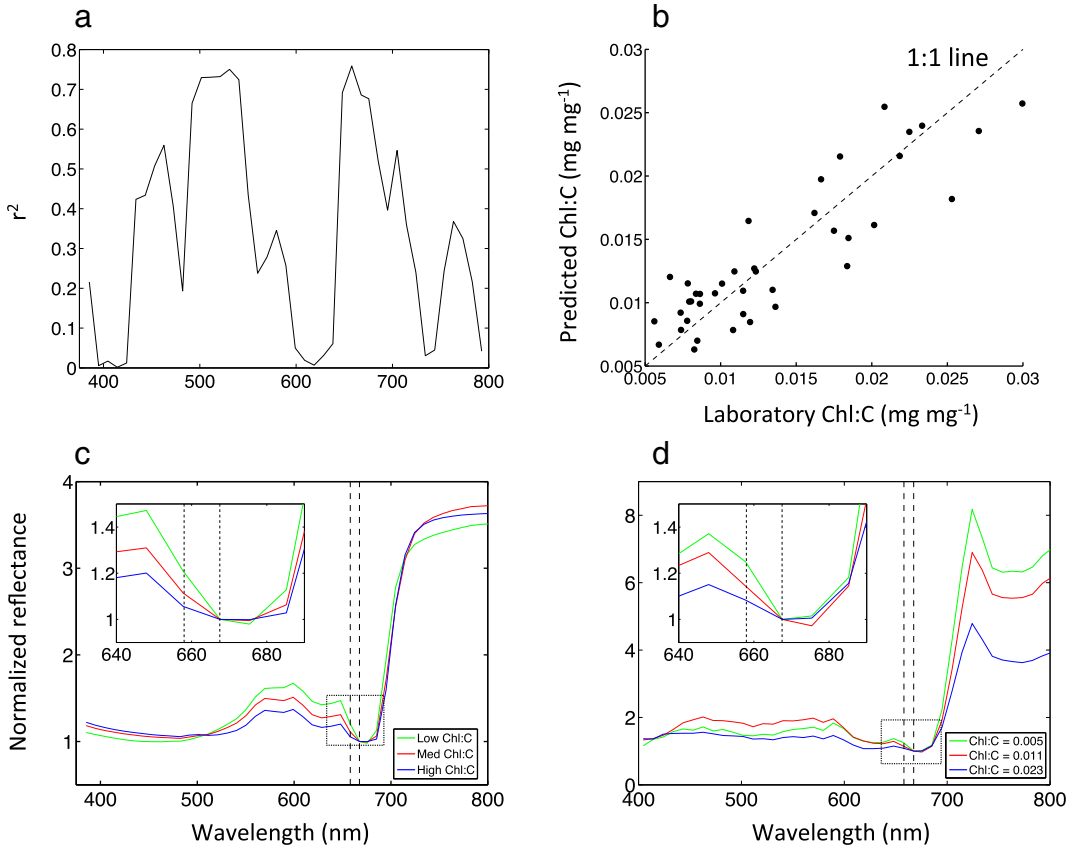

Fig. 1. (a) Variations in the coefficient of determination (r^2) by wavelength after regressing the first derivative of pseudoabsorbance against laboratory Chl:C using an exponential fit. (b) Scatterplot showing the relationship between laboratory measured Chl:C and predicted Chl:C ($r^2 = 0.76$) using a 5-fold cross validation. Chl:C was predicted using the empirical relationship between observed Chl:C and the first derivative of pseudoabsorbance between 658 and 667 nm. Dashed line shows 1:1 line. (c,d) Laboratory (c) and AVIRIS (d) reflectance spectra, normalized at 667 nm, showing differences in reflectance between blades and AVIRIS pixels of varying Chl:C. Area inside dashed lines show portion of the spectrum used for the estimation of Chl:C. Inset shows magnified area inside dotted box.

examined 17 time scales ranging from 0.5 yr. to 8 yr. Ninety-five percent confidence levels were calculated by using red noise spectra as background spectra to account for temporal autocorrelation in the data. Red-noise was modeled as a lag-1 autoregressive process (i.e., the correlation between the time series and itself, shifted by one season; Santos, Galvão, Suzuki, & Trigo, 2001). Wavelet analysis was performed on the time series of kelp biomass summed across the entire study area, and separately for kelp biomass north of Pt. Conception (central California) and kelp biomass south of Pt. Conception (southern California). Wavelet analysis indicated that variability in kelp biomass was dominated by a strong seasonal cycle. Therefore, we examined the timing and variability of the kelp canopy biomass seasonal cycle for each 500 m-coastline segment. At each site we identified the season in which annual maximums in biomass occurred most often (i.e., the mode of annual maximums) and the variability in the timing of annual maximums (i.e., the variation ratio, the proportion of years when biomass maximums did not occur in the modal season).

3. Results

3.1. Expected cloud-free HysPIRI coverage of global giant kelp habitat

The global distribution of giant kelp experienced varying levels of cloud coverage from 2001–2010. The percent of cloud free MODIS views over this time period ranged from 12 (Jan–Mar in the Falkland Islands) to 52 (Jan–Mar in South Africa). Assuming a 19-day repeat time for the VSWIR sensor, our results indicate that, on average, all regions except the sub-Antarctic Islands will have at least 1 cloud free HyspIRI view per season (Table 1). If HyspIRI is flown simultaneously with Landsat 8, the two sensors would be able to provide between 1 and 5 cloud free views per season of each region (Table 1).

3.2. Kelp canopy biomass dynamics

Wavelet analysis revealed statistically significant periodicity in kelp biomass fluctuations along the coast of California throughout most of study period (Fig. 2a,b). The power spectrum of this time series was dominated by modes of ~1-year (Fig. 2c), indicating that kelp biomass abundance experiences a strong seasonal cycle with a period of 1 year. However, there were substantial differences in kelp biomass variability between central and southern California (Figs. 3 and 4). Central California exhibited a consistent, highly significant periodicity dominated by a 1-year mode (Fig. 3b & c). The southern California time series displayed more transient seasonal dynamics (Fig. 4a). Statistically significant periodicity with a mode of 0.5–2 years was present from 1988–1995 and from 2003–2010 (Fig. 4b & c). The global wavelet spectrum for southern California exhibited a peak at a period of 2 years, which was not present in the central California spectrum. No significant seasonal periodicity was detected from 1996–2002 for southern California (Fig. 4a), highlighting the non-stationary behavior of kelp biomass dynamics in this region.

Overall, variability in the seasonal cycle of kelp biomass, measured using the variation ratio, was higher in southern California than in central California (Fig. 5). In central California, biomass consistently peaked during the fall (83% of sites in central California were characterized with fall maximums). In southern California, biomass maximums occurred most often during the winter for 13% of sites, during the spring for 35% of sites, during the summer for 36% of sites, and during the fall for 16% of sites.

3.3. Variability in kelp physiological condition

The mainland SBC kelp forest canopies showed high amounts of spatial variability in Chl:C of the surface canopy in April 2013 (Fig. 6a). Chl:C estimated from the AVIRIS imagery ranged from 0.005 to 0.025 mg mg^{-1}, with a mean Chl:C of 0.012 (0.003 s.d.) mg mg^{-1}. This is similar to the observed Chl:C mean and range of sampled mature, healthy canopy blades across all sample dates, which were 0.012 and 0.005–0.030 mg mg^{-1}, respectively. Chl:C was only estimated for pixels with a high proportion of emergent kelp canopy (canopy fractional cover of 0.4 as estimated by MESMA).

For this image, Chl:C concentrations were significantly correlated to bathymetry ($r = 0.41$, $p < 0.001$; Fig. 6b), but not pixel fractional cover of emergent kelp canopy ($r = -0.07$, $p = 0.29$; Fig. 6c).

4. Discussion

The temporal, spatial, and spectral characteristics of HyspIRI make this sensor particularly well suited to advance our understanding of giant kelp forest dynamics on local (<1 km) to global scales. Monitoring giant kelp populations is challenging because, compared to many habitat-structuring primary producers, giant kelp forests are exceptionally dynamic (see Variability in kelp canopy biomass below). In order to identify the processes that structure giant kelp population dynamics, researchers need observations of kelp populations that are both long-term and high frequency.

HyspIRI's planned 19-day VSWIR revisit time will enable the sensor to acquire at least 1 cloud free view per season of giant kelp habitat in nearly all regions of the world, thereby allowing us to resolve seasonal variability in giant kelp biomass and physiological condition (Table 1). This coverage will help researchers improve their understanding of the seasonal and interannual variability in giant kelp biomass and condition, the drivers of this variability, and its consequences for the ecosystem functioning of these forests. HyspIRI will help extend the record of remote kelp observations that is currently being built using historical Landsat imagery (Cavanaugh et al., 2011). If HyspIRI and a sensor such as Landsat 8 were both operational, we would be able to obtain between 3 and 5 observations of kelp canopy biomass per season for most of the regions that contain giant kelp. This approximately

Table 1
Expected mean (std dev.) number of cloud free HyspIRI and Landsat 8 views per season for the 8 giant kelp regions (following Graham et al., 2007). Expected cloud free views were calculated using the fraction of MODIS views that were cloud free from 2000–2010 for each region and the revisit times for HyspIRI (19 days) and Landsat 8 (16 days).

		Region						
	NW North America	SW North America	South America	Falkland Islands	South Africa	Tasmania	New Zealand	Sub-Antarctic Islands
HyspIRI only								
Jan–Mar	1.0 (0.2)	2.0 (0.5)	1.0 (0.6)	1.1 (0.2)	2.5 (0.8)	1.5 (0.4)	1.4 (0.4)	0.6 (0.3)
Apr–Jun	1.3 (0.3)	2.0 (0.5)	1.1 (0.4)	1.1 (0.3)	2.1 (0.6)	1.4 (0.4)	1.4 (0.4)	0.7 (0.3)
Jul–Sep	1.5 (0.6)	2.3 (0.7)	1.1 (0.3)	1.0 (0.2)	2.1 (0.6)	1.3 (0.4)	1.4 (0.4)	0.9 (0.4)
Oct–Dec	1.0 (0.2)	2.2 (0.6)	0.9 (0.5)	1.1 (0.2)	2.2 (0.7)	1.3 (0.3)	1.2 (0.3)	0.6 (0.2)
HyspIRI & Landsat 8								
Jan–Mar	2.2 (0.4)	4.4 (1.0)	2.1 (1.3)	2.5 (0.5)	5.4 (1.8)	3.2 (0.8)	3.0 (0.9)	1.3 (0.7)
Apr–Jun	2.9 (0.6)	4.3 (1.2)	2.4 (0.8)	2.3 (0.6)	4.6 (1.3)	3.0 (0.8)	3.0 (0.9)	1.6 (0.7)
Jul–Sep	3.4 (1.4)	4.9 (1.6)	2.4 (0.7)	2.2 (0.5)	4.6 (1.4)	2.9 (0.8)	3.0 (0.8)	1.9 (0.9)
Oct–Dec	2.1 (0.5)	4.8 (1.3)	1.9 (1.0)	2.5 (0.5)	4.8 (1.6)	2.8 (0.7)	2.6 (0.6)	1.3 (0.5)

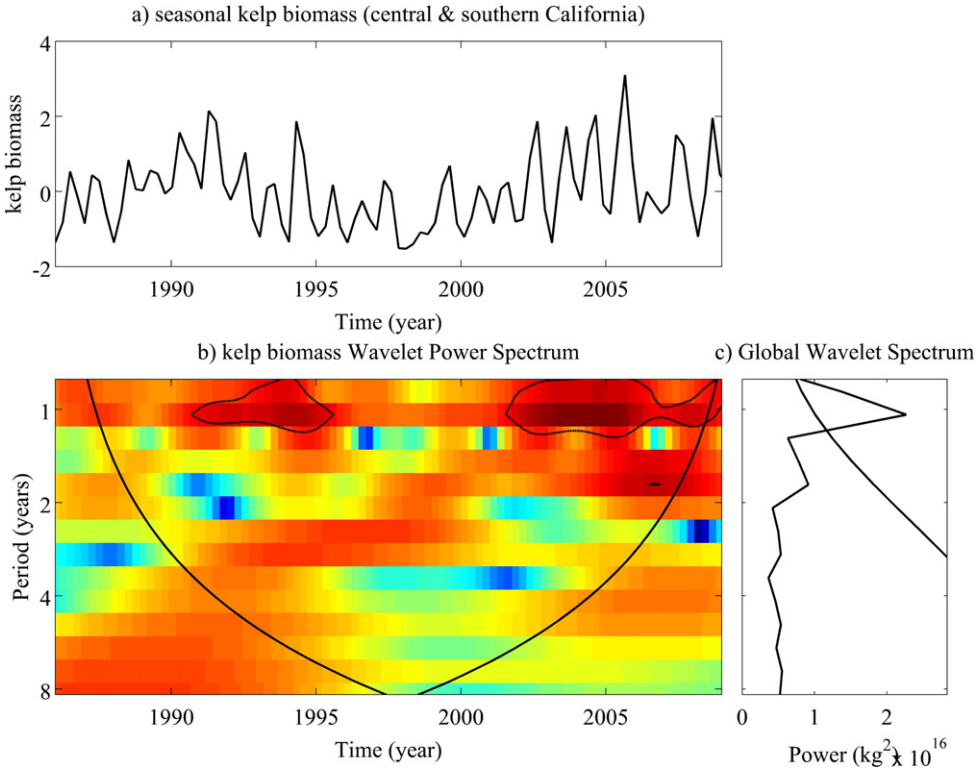

Fig. 2. (a) normalized (z-score) time series of seasonal giant kelp biomass for entire study area from Año Nuevo to the USA/Mexico border. (b) The local wavelet power spectrum of (a) using the Morlet wavelet. The contour lines enclose regions of greater than 95% confidence for a red-noise process. U-shaped curve indicates the "cone of influence", where edge effects become important. (c) Average wavelet power spectrum of the kelp biomass signal. Solid curve gives the 95% confidence level.

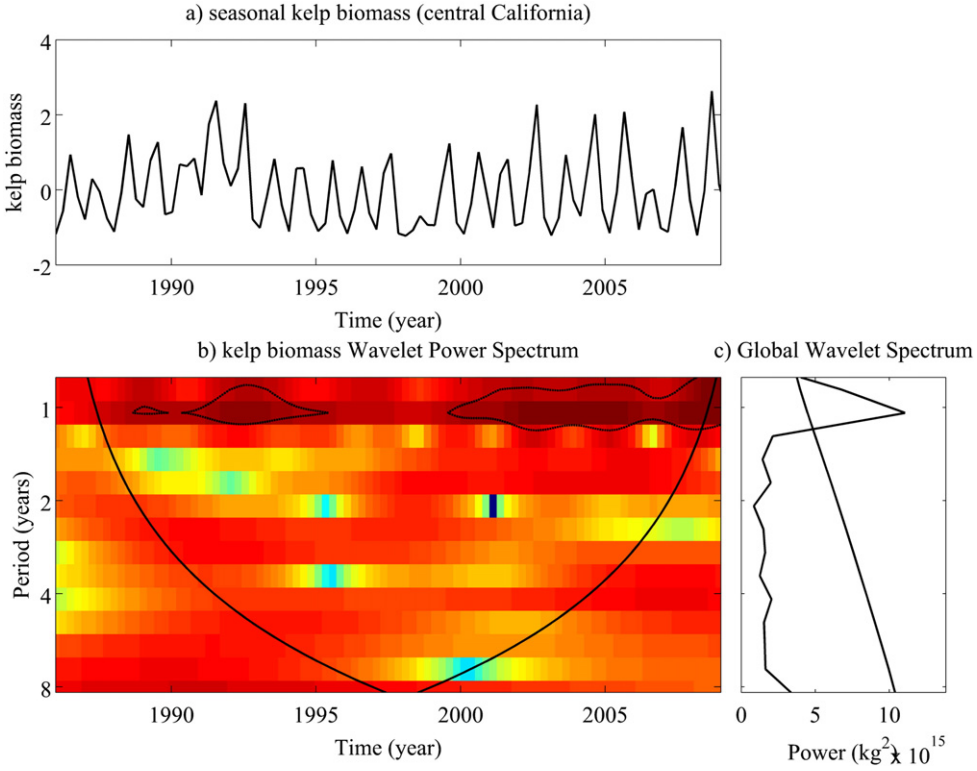

Fig. 3. (a) normalized (z-score) time series of seasonal giant kelp biomass for study area from Año Nuevo to Pt. Conception. (b) The local wavelet power spectrum of (a) using the Morlet wavelet. The contour lines enclose regions of greater than 95% confidence for a red-noise process. U-shaped curve indicates the "cone of influence", where edge effects become important. (c) Average wavelet power spectrum of the kelp biomass signal. Solid curve gives the 95% confidence level.

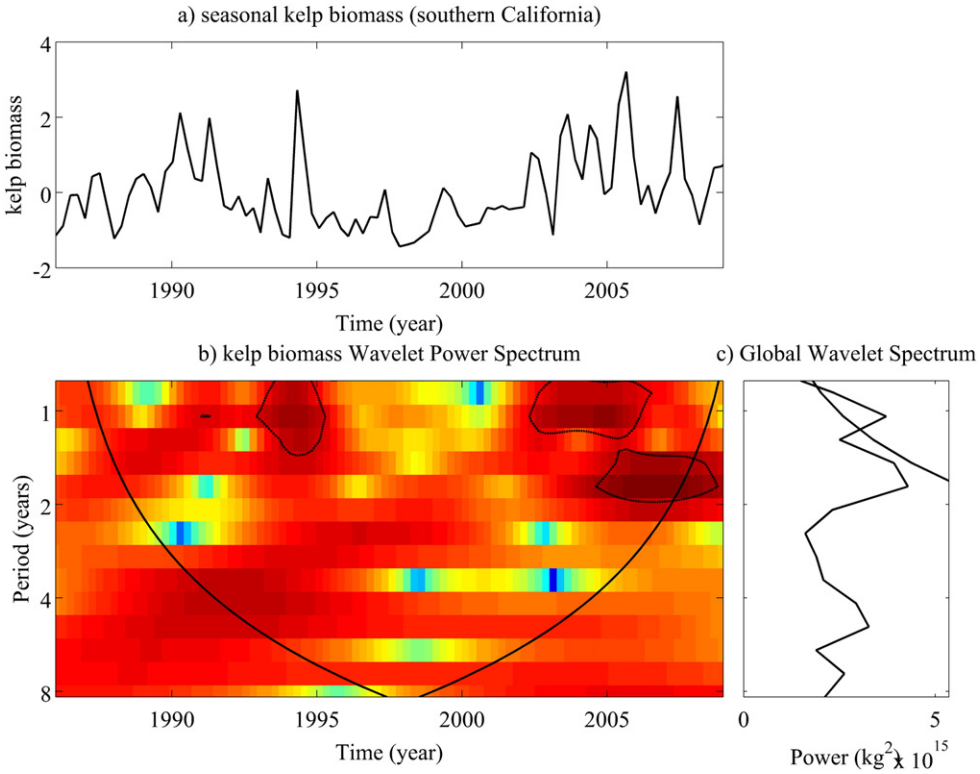

Fig. 4. (a) Normalized (z-score) time series of seasonal giant kelp biomass for study area south of Pt. Conception to the USA/Mexico border. (b) The local wavelet power spectrum of (a) using the Morlet wavelet. The contour lines enclose regions of greater than 95% confidence for a red-noise process. U-shaped curve indicates the "cone of influence", where edge effects become important. (c) Average wavelet power spectrum of the kelp biomass signal. Solid curve gives the 95% confidence level.

monthly coverage could be used to further refine our understanding of giant kelp biomass phenology. For example, discrete events such as wave disturbances are important drivers of giant kelp biomass dynamics. Higher temporal coverage would improve our ability to document the effects of these discrete events. Our estimates of seasonal cloud free coverage assumed 19- and 16-day revisit time (HyspIRI and Landsat 8 respectively) for all regions. In reality, the revisit times decrease poleward from the equator. As a result, our estimates of seasonal cloud free coverage are likely to be conservative.

Giant kelp typically occurs in large patches and HyspIRI's 60 m resolution will be sufficient to resolve patches >3600 m^2. A recent analysis of the metapopulation dynamics of giant kelp forests in southern California from Landsat 5 TM imagery found that 96% of the identified kelp patches were >3600 m^2 (Cavanaugh et al., 2014). Further work will be necessary to characterize kelp canopy detection limits using HyspIRI imagery. Researchers will be able to use techniques similar to those described in Cavanaugh et al. (2011) to measure canopy biomass from HyspIRI, however the coarser spatial resolution of HyspIRI as compared to Landsat may lead to biases in biomass estimates as patches that are distinguishable on 30 m resolution Landsat imagery may be undetectable with 60 m HyspIRI imagery. There is also the potential to use spectral unmixing techniques to address these biases and to identify patches <3600 m^2 because HyspIRI's signal to noise (S:N) levels will likely be greater than Landsat's S:N values, which may allow subpixel kelp patches to be quantified with higher accuracy.

4.1. Variability in kelp canopy biomass

Giant kelp biomass along the coast of California generally exhibits a seasonal cycle, however the strength and timing of this cycle vary a great deal in both space and time (Figs. 2–4). In central California biomass typically peaks in the fall and then declines rapidly during the winter. These winter declines are well correlated with wave disturbances (Bell et al., in press). The exposed coastline north of Pt. Conception experiences large magnitude storm disturbances each winter, which physically dislodge adult kelp plants and cause widespread mortality (Bell et al., in press; Reed et al., 2011). When the winter storm season ends, high levels of nutrients and light facilitate recruitment and recovery of kelp populations (Graham et al., 1997).

In contrast to central California, there is a great deal of spatial variability in the timing of annual biomass maximums in southern California (Fig. 5). In addition, periodicity in giant kelp biomass varies on interannual timescales (Fig. 4b). In southern California large magnitude storm disturbances occur less frequently, typically every 2 to 4 years (Bell et al., in press; Cavanaugh et al., 2011). In addition, the coastline of southern California presents a myriad of wave exposures, resulting in a large degree of spatial variability in the impact of swell events. This region also experiences spatiotemporal variability in upwelling and nutrient levels (Di Lorenzo, 2003; Otero & Siegel, 2004; Palacios, Hazen, Schroeder, & Bograd, 2013). The less frequent disturbance experienced in southern California may also enable biotic processes such as sea urchin grazing to play larger roles in structuring cycles in kelp abundance (Bell et al., in press). While our analysis of biomass variability was limited to California, previous studies have also documented high amounts of variability in New Zealand, Chile, and other parts of the world (Brown, Nyman, Keough, & Chin, 1997; Buschmann et al., 2004; Graham et al., 2007).

Previous studies have characterized seasonal cycles in giant kelp biomass and attributed those cycles to environmental controls such as nutrient levels, temperature stress, and wave disturbance (Clendenning, 1971; Hay, 1990; Jackson, 1977; Reed & Foster, 1984; Van Tussenbroek, 1993). However, these studies have generally been performed on local scales and do not examine the spatial variability in seasonal cycles. Giant kelp populations are influenced by processes acting over a wide variety of spatial and temporal scales (Bell et al., in press; Edwards, 2004). This variability has important implications for kelp forest monitoring. For example, each year the California Department of Fish and Wildlife conducts a statewide aerial kelp survey in the late summer/

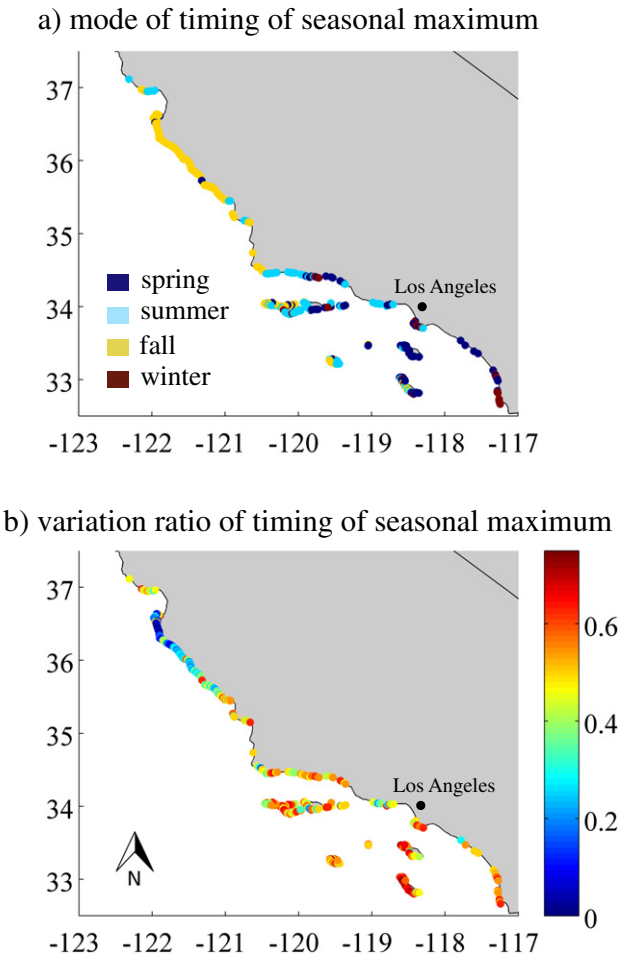

Fig. 5. (a) Season in which annual kelp biomass maximums occurred most often between 1984 and 2011 for each 500 m section of coastline. (b) Variation ratio of timing of seasonal maximums.

early fall to coincide with the timing kelp canopy maxima. While central California typically experiences biomass maxima during this time, southern California often does not (Fig. 5). Further analysis of the regional Landsat kelp biomass time series (Figs. 3a & 4a) shows that between 1986 and 2009, central California experienced annual biomass maxima during the fall in 21 out of 24 years while southern California experienced biomass maxima during the fall in only 4 out of 24 years. This spatial variability could lead to biases in regional comparisons of maximum kelp standing stock or in regional comparisons of annual kelp net primary production derived from single measurements of standing stock (Reed, Rassweiler, & Arkema, 2009).

Giant kelp's seasonal cycle has important ecological implications and improvements in our understanding of giant kelp seasonal variations may have important ramifications. Giant kelp is a foundation species, and in southern California, the abundance of giant kelp during the spring has been shown to impact the diversity and richness of kelp forest food webs during the subsequent summer (Byrnes et al., 2011). Giant kelp abundance also influences the net primary production and population dynamics of individuals in the kelp forest ecosystem (Reed et al., 2008).

For example, giant kelp is the preferential food source for red sea urchins, one of the most economically important species that inhabit kelp forests in California (Leighton, 1971). The gonads of the female urchins, whose size and quality are partially controlled by food supply, are harvested by fishermen just before spawning. The reproductive cycle of sea urchins generally follows an annual cycle, but, like kelp abundance, there is a large amount of spatial and temporal variability in spawning (Kato & Schroeter, 1985). It is therefore feasible that the spawning cycle of sea urchins is impacted by the seasonal cycle of kelp abundance.

Future climate change is likely to result in phenological changes for many species, and these impacts may be especially pronounced in coastal and marine ecosystems (Edwards & Richardson, 2004). For example, there is evidence that the frequency of extreme wave heights in the northeast Pacific Ocean has increased in recent decades (Menéndez, Méndez, Losada, & Graham, 2008; Ruggiero, Komar, & Allan, 2010). These types of changes will undoubtedly have significant impacts on coastal ecosystem structure and function. Global observations of coastal ecosystems such as giant kelp forests on seasonal time scales will enable researchers to track phenological changes and improve our understanding of the drivers of these changes.

4.2. Variability in kelp physiological condition

The dynamic environment of the California coast leads to changes in the physiological state of the giant kelp canopy throughout the year. Elemental analysis of kelp blades in the SBC shows that blade organic nitrogen follows a similar pattern as available nitrate in the water column, while blade carbon remains relatively constant through the year (Brzezinski et al., 2013). This leads to elevated C:N during the summer and fall, when many kelp fronds lack active growing tips, blades become lighter in color, and photosynthetic rates decline (Clendenning, 1971). Increased ambient NO_3 concentrations and decreased PAR flux are known to positively influence the concentrations of photosynthetic pigments in giant kelp (e.g., Shivji, 1985). The nitrogen and pigment status of the giant kelp canopy changes seasonally and may be subject to the fluctuations in nutrient delivery to the inner shelf, thus it is critical to measure these indicators of physiological state at timescales relevant to the dynamics of the local environment. Measurements of kelp pigments and nutrient status at a few sites are not sufficient to explain these patterns on the scales of environmental variability affecting giant kelp populations.

Estimates of Chl:C from April 2013 AVIRIS reflectance image showed a high amount of spatial variability, ranging from 0.005 to 0.025 mg mg^{-1} over distance of about 15 km (Fig. 6a). The observed spatial variability underscores the importance of developing a time series of physiological condition over appropriate spatial and temporal scales. Variability in Chl:C is significantly and positively correlated with changes in depth. This relationship may indicate that the physiological condition for the surface kelp canopy (higher Chl:C values) may be improved for individuals attached to deeper areas of the reef (Fig. 6b). Giant kelp can occupy different nutrient environments not only over regional scales, but also over a reef scale, as thalli with deeper holdfasts may be able to access greater amounts of nitrogen. Parnell et al. (2010) found that the depth of the 25.1 σ_T isopycnal, which is associated with the threshold NO_3 concentration for kelp growth, accounted for 71% of the variability in kelp density near Pt. Loma, CA. Kelp plants at greater depths may occupy nutrient refugia that may lead to a higher quality surface canopy. The spatial differences may also be a factor of the age structure of the canopy fronds. Variation in the production and growth of fronds in different nutrient and light conditions, coupled with intrinsic frond senescence, may lead to variability in age structure, pigment concentration, and photosynthetic performance. Clearly, the environment of the entire plant can have an effect on the condition of the canopy and there is much work to done on relating bathymetric variability to changes in giant kelp canopy processes.

Previous work focusing on giant kelp pigments has investigated the role of changing magnitudes and distributions of light energy along a depth gradient and its role on photosynthetic performance (Colombo-Pallotta, García-Mendoza, & Ladah, 2006; Edwards & Kim, 2010; Wheeler, 1980); however there has been little research studying these changes through time or across seascapes. Changes in photosynthetic

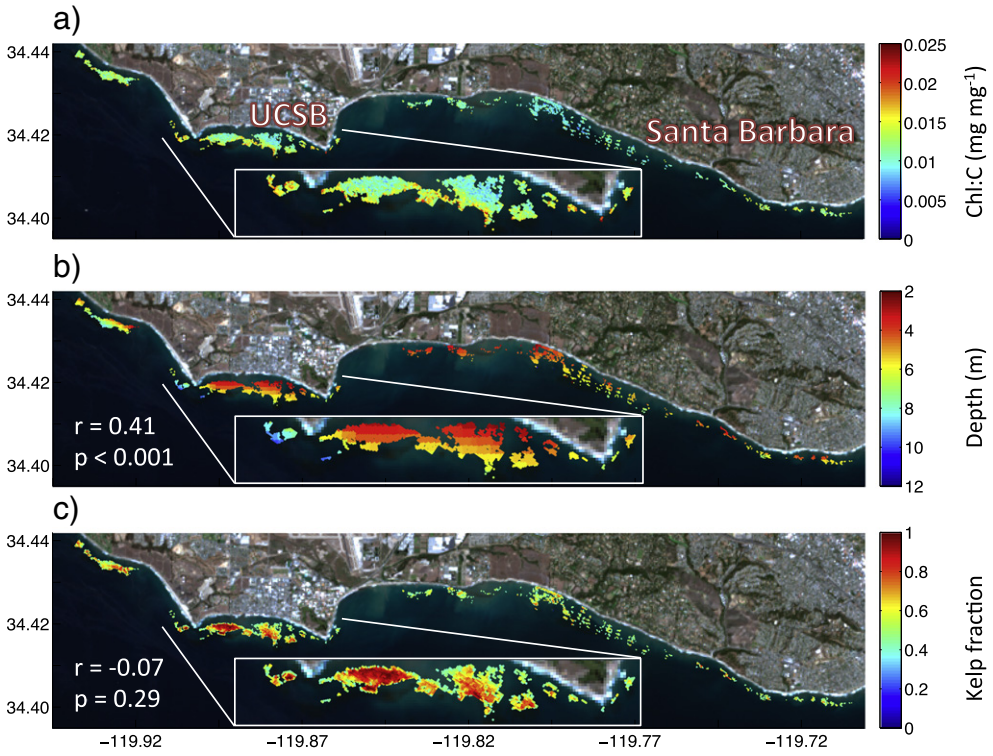

Fig. 6. Map of the distribution of (a) estimated Chl:C in the surface canopy (b) depth and (c) kelp pixel fraction of Santa Barbara area kelp forests on April 11th, 2013. Insets show magnified data of the Isla Vista kelp forest and reef. Data for a. and c. from AVIRIS hyperspectral images, and b. from NOAA National Geophysical Data Center coastal relief model (Divins & Metzger, 2009).

performance and kelp primary production rates would likely alter energy flows and change interaction strengths within the kelp forest food web (e.g., Byrnes et al., 2011). Deterioration of kelp fronds associated with low nutrient conditions may be a result of decreased physiological condition, and could potentially have effects on the ability of the kelp to provide structure and withstand disturbances.

The remote estimation of physiological condition from hyperspectral images presents several unique challenges. For one, remote sensing in nearshore environments embodies a number of sources of noise in reflectance spectra (cf., sunglint, phytoplankton blooms, sediment runoff, etc.). Kelp forests do not significantly dampen long-period, swell waves, but they can dampen shorter wavelength wind waves (Elwany, O'Reilly, Guza, & Flick, 1995; Seymour, 1996). Under calm ocean conditions, kelp forests often reduce observed sun glint (see Fig. 1 in Roberts, Quattrochi, Hulley, Hook, & Green, 2012), but are still subject to sky glint. In addition, NIR radiation is rapidly attenuated by water and the giant kelp canopy reflectance signal can be dramatically reduced if the canopy is even slightly submerged. This has the potential to reduce the accuracy of estimates of kelp canopy biomass and physiological state. However, Cavanaugh et al. (2011) found that tides and currents did not significantly impact remote estimates of canopy biomass for the 3 sampled kelp beds off the coast of Santa Barbara, as vertical tidal fluctuations and current speeds were relatively small (Fram et al., 2008). These processes may play greater roles in other regions (Britton-Simmons, Eckman, & Duggins, 2008).

The increased spectral resolution and dynamic range of HypsIRI as compared to Landsat 5 TM should allow for improved canopy biomass estimation. The spectral bands and dynamic range of Landsat TM observations required the use of a single kelp endmember for all images in spectral mixing modeling (Cavanaugh et al., 2011). This limits the ability to correct for changes in physiological state during biomass estimation from Landsat TM imagery. The use of a single kelp endmember may be responsible for a substantial fraction of the unexplained variance when relating the estimated fraction of kelp in each pixel to field biomass measurements (Cavanaugh et al., 2011). HypsIRI could allow for the use of multiple kelp endmembers that represent a variety of physiological states.

4.3. Future directions

Recent advances in the remote estimation of giant kelp canopy biomass from multispectral sensors such as Landsat 5 TM have provided valuable insight into the processes that control the abundance, productivity, and food web structure of giant kelp forests (Bell et al., in press; Byrnes et al., 2011; Cavanaugh et al., 2011, 2013, 2014; Reed et al., 2011). However, this research has only examined giant kelp forests along the coast of California. These techniques can be applied to giant kelp forests in other parts of the world (Tasmania, Chile, South Africa, Falkland Islands, sub-Antarctic islands, etc.) enabling cross-regional comparisons. For example, during recent decades there has been a dramatic decline in giant kelp along the coast of eastern Tasmania (Johnson et al., 2011). Multi-temporal satellite imagery could be used to comprehensively quantify the magnitude, extent, and timing of this decline and examine its drivers. Local studies have documented climate change related impacts on kelp forests in nearly every region of the globe (Bolton, Anderson, Smit, & Rothman, 2012; Johnson et al., 2011; Moy & Christie, 2012; Wernberg et al., 2010). Easily accessible, global, long-term satellite datasets would facilitate a global analysis of the impacts on climate change on giant kelp forest ecosystems.

The application of hyperspectral imagery to detect changes in the physiological condition of giant kelp is the next logical step in understanding submerged and emergent vegetation population dynamics from satellite observations. There is a great need for the development and validation of hyperspectral indices that can be used to estimate nutrient and pigment concentrations of aquatic vegetation in general and of giant kelp in particular. These concentrations can then be linked to characteristics such as age, canopy morphology, light exposure, photosynthetic yield, etc. This information may enable more accurate

predictions of biomass dynamics. For example, recent work suggests that the probability of giant kelp frond mortality is highly dependent on frond age, which will allow researchers to separate losses due to disturbance vs. senescence (Rodriguez et al., 2013). Remote measurements of physiological state may also prove useful for understanding the controls on range limits. Biogeographic theory predicts that a species abundance and fitness peaks in the center of its range and declines toward its range edge as environmental conditions become unfavorable (Brown, 1984; Hengeveld & Haeck, 1982; Huey, 1991). However, the prevalence of this pattern has been questioned (Sagarin & Gaines, 2002). Measures of photosynthetic performance across the entire ranges of species such as giant kelp could be used to test this theory, identify the environmental variables that set range limits, and predict how climate change might impact these limits. Global, hyperspectral imagery with high temporal resolution (seasonal or greater) would greatly enhance our understanding of the dynamics of these important ecosystems.

Acknowledgments

We acknowledge support from the Santa Barbara Coastal LTER, funded by the US National Science Foundation (OCE 0620276 & 1232779), the NASA grant #NNX12AP08G, and also by NASA grant NNX14AR62A as part of the Biodiversity and Ecological Forecasting program. We also acknowledge the NASA Earth and Space Science Fellowship Program for supporting both T.W.B. and K.C.C. Also, deep gratitude is extended to Shannon Herrer and Clint Nelson of the SBC LTER for field collection and laboratory analysis, Dr. Norm Nelson of the Earth Research Institute for teaching laboratory techniques, and Dr. Michael Mercury for providing the MODIS 5 km daytime cloud mask dataset. We also especially thank Dan Reed for advice and assistance, as well as leading the SBC LTER project. We also thank guest editor Eric Hochberg and two anonymous reviewers from thoughtful comments that have improved the manuscript.

References

Augenstein, E., Stow, D., & Hope, A. (1991). Evaluation of SPOT HRV-XS data for kelp resource inventories. *Photogrammetric Engineering and Remote Sensing*, *57*(5), 501–509.

Behrenfeld, M.J., Boss, E., Siegel, D.A., & Shea, D.M. (2005). Carbon-based ocean productivity and phytoplankton physiology from space. *Global Biogeochemical Cycles*, *19*(1), 1–14http://dx.doi.org/10.1029/2004GB002299.

Bell, T.W., Cavanaugh, K.C., Reed, D.C., & Siegel, D.A. (2015). Geographical variability in the controls of giant kelp biomass dynamics. *Journal of Biogeography*, Advance online publication. http://dx.doi.org/10.1111/jbi.12550 (in press).

Bolton, J., Anderson, R., Smit, A., & Rothman, M. (2012). South African kelp moving eastwards: The discovery of *Ecklonia maxima* (Osbeck) Papenfuss at De Hoop Nature Reserve on the south coast of South Africa. *African Journal of Marine Science*, *34*, 147–151.

Britton-Simmons, K., Eckman, J.E., & Duggins, D.O. (2008). Effect of tidal currents and tidal stage on estimates of bed size in the kelp Nereocystis luetkeana. *Marine Ecology Progress Series*, *355*, 95–105.

Brown, J.H. (1984). On the relationship between abundance and distribution of species. *American Naturalist*, 255–279.

Brown, M.T., Nyman, M.A., Keough, J.A., & Chin, N.K.M. (1997). Seasonal growth of the giant kelp *Macrocystis pyrifera* in New Zealand. *Marine Biology*, *129*, 417–424.

Brzezinski, M., Reed, D., & Harrer, S. (2013). Multiple sources and forms of nitrogen sustain year-round kelp growth on the inner continental shelf of the Santa Barbara channel. *Oceanography*, *26*, 114–123.

Buschmann, A.H., Väsquez, J.A., Osorio, P., Reyes, E., Filún, L., Hernández-González, M.C., et al. (2004). The effect of water movement, temperature and salinity on abundance and reproductive of patterns of *Macrocystis* spp. (Phaeophyta) at different latitudes in Chile. *Marine Biology*, *145*, 849–862.

Bushing, W.W. (1997). GIS-based gap analysis of an existing marine reserve network around Santa Catalina Island. *International Journal of Marine Geodesy*, *20*, 205–234.

Byrnes, J., Reed, D., Cardinale, B., Cavanaugh, K., Holbrook, S., & Schmitt, R. (2011). Climate driven increases in storm frequency simplify kelp forest food webs. *Global Change Biology*, *17*, 2513–2524.

Castorani, C.N., Reed, D.C., Alberto, F., Bell, T.W., Simons, R.D., Cavanaugh, K.C., et al. (2015). Connectivity structures local population dynamics: a long-term, large-scale empirical test in a marine metapopulation. *Ecology* (in press).

Cavanaugh, K.C., Kendall, B.E., Siegel, D.A., Reed, D.C., Alberto, F., & Assis, J. (2013). Synchrony in dynamics of giant kelp forests is driven by both local recruitment and regional environmental controls. *Ecology*, *94*(2), 499–509.

Cavanaugh, K.C., Siegel, D.A., Kinlan, B., & Reed, D.C. (2010). Scaling giant kelp field measurements to regional scales using satellite observations. *Marine Ecology Progress Series*, *403*, 13–27.

Cavanaugh, K.C., Siegel, D.A., Raimondi, P.T., & Alberto, F. (2014). Patch definition in metapopulation analysis: a graph theory approach to solve the mega-patch problem. *Ecology*, *95*, 316–328.

Cavanaugh, K.C., Siegel, D.A., Reed, D.C., & Dennison, P.E. (2011). Environmental controls of giant-kelp biomass in the Santa Barbara Channel, California. *Marine Ecology Progress Series*, *429*, 1–17.

Cazelles, B., Chavez, M., Berteaux, D., Ménard, F., Vik, J.O., Jenouvrier, S., et al. (2008). Wavelet analysis of ecological time series. *Oecologia*, *156*, 287–304.

Clendenning, K.A. (1971). Photosynthesis and general development. In W.J. North (Ed.), *The Biology of Giant Kelp Beds (Macrocystis) in California. Beihefte Zur Nova Hedwigia*. Lehre, Germany: Verlag Von J. Cramer (Coley).

Colombo-Pallotta, M.F., García-Mendoza, E., & Ladah, L.B. (2006). Photosynthetic performance, light absorption, and pigment composition of *Macrocystis pyrifera* (Laminariales, Phaeophyceae) blades from different depths. *Journal of Phycology*, *42*(6), 1225–1234.

Dayton, P., & Tegner, M.J. (1984). Catastrophic storms, El Niño, and patch stability in a southern California kelp community. *Science*, *224*, 283–285.

Dayton, P., Tegner, M., Edwards, P., & Riser, K. (1999). Temporal and spatial scales of kelp demography: The role of oceanographic climate. *Ecological Monographs*, *69*, 219–250.

Deysher, L.E. (1993). Evaluation of remote sensing techniques for monitoring giant kelp populations. *Hydrobiologia*, *260–261*(1), 307–312.

Di Lorenzo, E. (2003). Seasonal dynamics of the surface circulation in the Southern California Current System. *Deep Sea Research Part II: Topical Studies in Oceanography*, *50*, 2371–2388.

Di Lorenzo, E., Cobb, K.M., Furtado, J.C., Schneider, N., Anderson, B.T., Bracco, A., et al. (2010). Central Pacific El Niño and decadal climate change in the North Pacific Ocean. *Nature Geoscience*, *3*(11), 762–765.

Divins, D.L., & Metzger, D. (2009). NGDC coastal relief model. http://www.ngdc.noaa.gov/mgg/coastal/coastal.html

Donnellan, M. (2004). *Spatial and temporal variability of kelp forests canopies in central California.* (MS Thesis) San Jose, CA: San Jose State University.

Edwards, M. (2004). Estimating scale-dependency in disturbance impacts: El Niños and giant kelp forests in the northeast Pacific. *Oecologia*, *138*, 436–447. http://dx.doi.org/10.1007/s00442-003-1452-8.

Edwards, M., & Kim, K. (2010). Diurnal variation in relative photosynthetic performance in giant kelp *Macrocystis pyrifera* (Phaeophyceae, Laminariales) at different depths as estimated using. *Aquatic Botany*, *92*(2), 119–128.

Edwards, M., & Richardson, A.J. (2004). Impact of climate change on marine pelagic phenology and trophic mismatch. *Nature*, *430*(7002), 881–884.

Elwany, M.H.S., O'Reilly, W.C., Guza, R.T., & Flick, R.E. (1995). Effects of Southern California kelp beds on waves. *Journal of Waterway, Port, Coastal, and Ocean Engineering*, *121*(2), 143–150.

Foster, M., & Schiel, D. (1985). Ecology of giant kelp forests in California: A community profile. *FWS/OBS-85 (7.2), San Jose State Univ., Moss Landing, CA (USA)*. Moss Landing Marine Labs.

Fram, J.P., Stewart, H.L., Brzezinski, M.A., Gaylord, B., Reed, D.C., Williams, S.L., et al. (2008). Physical pathways and utilization of nitrate supply to the giant kelp, *Macrocystis pyrifera*. *Limnology and Oceanography*, *53*(4), 1589–1603.

Gagnon, P., Scheibling, R.E., Jones, W., & Tully, D. (2008). The role of digital bathymetry in mapping shallow marine vegetation from hyperspectral image data. *International Journal of Remote Sensing*, *29*(3), 879–904.

Gao, B.C., Heidebrecht, K.B., & Goetz, A.F.H. (1993). Derivation of scaled surface reflectances from AVIRIS data. *Remote Sensing of Environment*, *44*, 165–178.

Geider, R.J. (1987). Light and temperature dependence of the carbon to chlorophyll a ratio in microalgae and cyanobacteria. *New Phytologist*, *106*(1), 1–34.

Geider, R.J., MacIntyre, H.L., & Kana, T.M. (1997). Dynamic model of phytoplankton growth and acclimation: responses of the balanced growth rate and the chlorophyll a: carbon ratio to light, nutrient-limitation and temperature. *Marine Ecology Progress Series*, *148*, 187–200.

Graham, M.H. (2004). Effects of local deforestation on the diversity and structure of Southern California giant kelp forest food webs. *Ecosystems*, *7*(4), 341–357.

Graham, M.H., Halpern, B., & Carr, M. (2008). *Diversity and dynamics of Californian subtidal kelp forests.* Food webs and the dynamics of marine benthic ecosystems, 103–134.

Graham, M.H., Harrold, C., Lisin, S., Light, K., Watanabe, J.M., & Foster, M.S. (1997). Population dynamics of giant kelp *Macrocystis pyrifera* along a wave exposure gradient. *Marine Ecology-Progress Series*, *148*, 269–279.

Graham, M.H., Vasquez, J., & Buschmann, A. (2007). Global ecology of the giant kelp *Macrocystis*: From ecotypes to ecosystems. *Oceanography and Marine Biology: An Annual Review*, *45*, 39–88.

Harms, S., & Winant, C. (1998). Characteristic patterns of the circulation in the Santa Barbara Channel. *Journal of Geophysical Research*, *103*, 3041–3065.

Hay, C.H. (1990). The distribution of *Macrocystis* (Phaeophyta: Laminariales) as a biological indicator of cool sea surface temperature, with special reference to New Zealand waters. *Journal of the Royal Society of New Zealand*, *20*, 313–336.

Hengeveld, R., & Haeck, J. (1982). The distribution of abundance. I. Measurements. *Journal of Biogeography*, 303–316.

Huey, R.B. (1991). Physiological consequences of habitat selection. *American Naturalist*, S91–S115.

Jackson, G.A. (1977). Nutrients and production of giant kelp, *Macrocystis pyrifera*, off Southern California. *Limnology and Oceanography*, *22*, 979–995.

Jamison, D.W. (1971). Aerial remote sensing as a tool in seaweed surveys. *International Symposium on Seaweed Research, 7th, Sapporo. Vol. 1971*.
Jensen, J., Estes, J., & Tinney, L. (1980). Remote-sensing techniques for kelp surveys. *Photogrammetric Engineering and Remote Sensing*, *46*(6), 743–755.
Johnson, C.R., Banks, S.C., Barrett, N.S., Cazassus, F., Dunstan, P.K., Edgar, G.J., et al. (2011). Climate change cascades: Shifts in oceanography, species' ranges and subtidal marine community dynamics in eastern Tasmania. *Journal of Experimental Marine Biology and Ecology*, *400*, 17–32.
Kato, S., & Schroeter, S.C. (1985). Biology of the red sea urchin, *Strongylocentrotus franciscanus*, and its fishery in California. *Marine Fisheries Review*, *47*, 1–20.
Larson, M.L., & McPeak, R.H. (1995). *Final environmental document, giant and bull kelp commercial and sportfishing regulations: Section 30 and 165, Title 14, California Code of Regulations*. Sacramento, CA: The Resources Agency.
Leet, W.S., Dewees, C.M., Klingbeil, R., & Johnson, E.J. (2001). *California's living marine resources: A status report*. State of CA Resources Agency and Fish and Game (593 pp.).
Leighton, D. (1971). Grazing activities of benthic invertebrates in southern California kelp beds. In W.J. North (Ed.), *The biology of giant kelp beds (Macrocystis) in California* (pp. 421–453). Lehre, Germany: Nova Hedwigia Verlag.
Lynn, R.J., & Simpson, J.J. (1987). The California current system: The seasonal variability of its physical characteristics. *Journal of Geophysical Research: Oceans (1978–2012)*, *92*, 12947–12966.
Mann, K.H. (1973). Seaweeds: Their productivity and strategy for growth. *Science*, *182*, 975–981.
Mantua, N., & Hare, S. (2002). The Pacific decadal oscillation. *Journal of Oceanography*, *58*, 35–44.
McPeak, R.H., Glantz, D.A., & Shaw, C.R. (1988). *The Amber forest. Beauty and biology of California's submarine forests*. San Diego, CA, USA: Westport Publishing.
McPhee-Shaw, E.E., Siegel, D.A., Washburn, L., Brzezinski, M.A., Jones, J.L., Leydecker, A., et al. (2007). Mechanisms for nutrient delivery to the inner shelf: Observations from the Santa Barbara Channel. *Limnology and Oceanography*, *52*(5), 1748–1766.
Menéndez, M., Méndez, F.J., Losada, I.J., & Graham, N.E. (2008). Variability of extreme wave heights in the northeast Pacific Ocean based on buoy measurements. *Geophysical Research Letters*, *35*(22).
Mercury, M., Green, R., Hook, S., Oaida, B., Wu, W., Gunderson, A., et al. (2012). Global cloud cover for assessment of optical satellite observation opportunities: A HyspIRI case study. *Remote Sensing of Environment*, *126*, 62–71.
Moy, F.E., & Christie, H. (2012). Large-scale shift from sugar kelp (Saccharina latissima) to ephemeral algae along the south and west coast of Norway. *Marine Biology Research*, *8*, 309–321.
North, W.J. (1991). The kelp beds of San Diego and Orange Counties. *Report to the San Diego Regional Water Quality Control Board* (270 pp.).
North, W.J., James, D.E., & Jones, L.G. (1993). History of kelp beds (Macrocystis) in Orange and San Diego Counties, California. *Hydrobiologia*, *260*, 277–283.
O'Reilly, W., & Guza, R. (1993). A comparison of two spectral wave models in the Southern California Bight. *Coastal Engineering*, *19*, 263–282.
Otero, M., & Siegel, D. (2004). Spatial and temporal characteristics of sediment plumes and phytoplankton blooms in the Santa Barbara Channel. *Deep Sea Research Part II: Topical Studies in Oceanography*, *51*, 1129–1149.
Palacios, D.M., Hazen, E.L., Schroeder, I.D., & Bograd, S.J. (2013). Modeling the temperature–nitrate relationship in the coastal upwelling domain of the California Current. *Journal of Geophysical Research, Oceans*, *118*(7), 3223–3239.
Parnell, P.E., Miller, E.F., Lennert-Cody, C.E., Dayton, P.K., & Carter, M.L. (2010). The response of giant kelp (*Macrocystis pyrifera*) in southern California to low-frequency climate forcing. *Limnology and Oceanography*, *55*, 2686–2702.
Reed, D.C., & Foster, M.S. (1984). The effects of canopy shadings on algal recruitment and growth in a giant kelp forest. *Ecology*, *65*, 937–948.
Reed, D.C., Rassweiler, A., & Arkema, K. (2008). Biomass rather than growth rate determines variation in net primary production by giant kelp. *Ecology*, *89*, 2493–2505.
Reed, D.C., Rassweiler, A., & Arkema, K. (2009). Density derived estimates of standing crop and net primary production in the giant kelp *Macrocystis pyrifera*. *Marine Biology*, *156*(10), 2077–2083.
Reed, D.C., Rassweiler, A., Carr, M.H., Cavanaugh, K.C., Malone, D.P., & Siegel, D.A. (2011). Wave disturbance overwhelms top-down and bottom-up control of primary production in California kelp forests. *Ecology*, *92*, 2108–2116.
Roberts, D.A., Gardner, M., Church, R., Ustin, S., Scheer, G., & Green, R. (1998). Mapping chaparral in the Santa Monica Mountains using multiple endmember spectral mixture models. *Remote Sensing of Environment*, *65*, 267–279.
Roberts, D.A., Quattrochi, D.A., Hulley, G.C., Hook, S.J., & Green, R.O. (2012). Synergies between VSWIR and TIR data for the urban environment: An evaluation of the potential for the Hyperspectral Infrared Imager (HyspIRI) Decadal Survey mission. *Remote Sensing of Environment*, *117*, 83–101.
Rodriguez, G.E., Rassweiler, A., Reed, D.C., & Holbrook, S.J. (2013). The importance of progressive senescence in the biomass dynamics of giant kelp (*Macrocystis pyrifera*). *Ecology*, *94*, 1848–1858.
Ruggiero, P., Komar, P.D., & Allan, J.C. (2010). Increasing wave heights and extreme value projections: The wave climate of the US Pacific Northwest. *Coastal Engineering*, *57*(5), 539–552.
Sagarin, R.D., & Gaines, S.D. (2002). Geographical abundance distributions of coastal invertebrates: Using one-dimensional ranges to test biogeographic hypotheses. *Journal of Biogeography*, *29*, 985–997.
Santos, C., Galvão, C., Suzuki, K., & Trigo, R. (2001). Matsuyama city rainfall data analysis using wavelet transform. *Annual Journal of Hydraulic Engineering*, *45*, 211–216.
SCCWRP (2011). *Status of the Kelp Beds 2011, San Diego and Orange Counties. Region Nine Kelp Survey Consortium.* Prepared by Costa Mesa, CA, USA: MBC Applied Environmental Sciences.
Seely, G., Duncan, M., & Vidaver, W. (1972). Preparative and analytical extraction of pigments from brown algae with dimethyl sulfoxide. *Marine Biology*, *12*, 184-188.
Seymour, R.J. (1996). Effects of Southern California kelp beds on waves, discussion. *Journal of Waterway, Port, Coastal, and Ocean Engineering*, *122*, 207–208.
Seymour, R.J. (1998). Effects of El Niños on the west coast wave climate. *Shore & Beach*, *66*, 3–6.
Seymour, R.J. (2011). Evidence for changes to the northeast Pacific wave climate. *Journal of Coastal Research*, *27*, 194–201.
Shivji, M. (1985). Interactive effects of light and nitrogen on growth and chemical composition of juvenile *Macrocystis pyrifera* (L.) C. At. (Phaeophyta) sporophytes. *Journal of Experimental Marine Biology and Ecology*, *89*, 81–96.
Sims, D.A., & Gamon, J.A. (2002). Relationships between leaf pigment content and spectral reflectance across a wide range of species, leaf structures and developmental stages. *Remote Sensing of Environment*, *81*(2–3), 337–354.
Stekoll, M.S., Deysher, L.E., & Hess, M. (2006). A remote sensing approach to estimating harvestable kelp biomass. *Journal of Applied Phycology*, *18*(3–5), 323–334.
Torrence, C., & Compo, G.P. (1998). A practical guide to wavelet analysis. *Bulletin of the American Meteorological Society*, *79*, 61–78.
Van Tussenbroek, B. (1993). Plant and frond dynamics of the giant kelp, *Macrocystis pyrifera*, forming a fringing zone in the Falkland Islands. *European Journal of Phycology*, *28*, 161–165.
Veisze, P., Kilgore, A., & Lampinen, M. (2001). Building a California kelp knowledge database using GIS. *Proc 2001 ESRI Education User Conf. ESRI paper*, *900*. San Diego, CA: ESRI.
Volent, Z., Johnsen, G., & Sigernes, F. (2007). Kelp forest mapping by use of airborne hyperspectral imager. *Journal of Applied Remote Sensing*, *1*(1), 011503.
Wernberg, T., Thomsen, M.S., Tuya, F., Kendrick, G.A., Staehr, P.A., & Toohey, B.D. (2010). Decreasing resilience of kelp beds along a latitudinal temperature gradient: Potential implications for a warmer future. *Ecology Letters*, *13*, 685–694.
Wessel, P., & Smith, W.H.F. (1996). A global, self-consistent, hierarchical, high-resolution shoreline database. *Journal of Geophysical Research, Solid Earth*, *101*, 8741–8743.
Wheeler, W. (1980). Pigment content and photosynthetic rate of the fronds of *Macrocystis pyrifera*. *Marine Biology*, *56*(2), 97–102.
Yoder, B., & Pettigrew-Crosby, R. (1995). Predicting nitrogen and chlorophyll content and concentrations from reflectance spectra (400–2500 nm) at leaf and canopy scales. *Remote Sensing of Environment*, *53*, 199–211.